JOC The Journal of Organic Chemistry

Article

pubs.acs.org/joc

Catalytic Asymmetric 5-*enolexo* Aldolizations. A Computational Study

Miglena K. Georgieva, Filipe J. S. Duarte, Margarida V. B. Queirós, and A. Gil Santos*

REQUIMTE, CQFB, Departamento de Química, Faculdade de Ciências e Tecnologia, Universidade Nova de Lisboa, 2829-516 Caparica, Portugal

Supporting Information

ABSTRACT: The diastereo- and enantioselectivity obtained experimentally by Enders et all. (Enders, D.; Niemeier, O.; Straver, S. *Synlett* **2006**, 3399−3402) in the amine-catalyzed intramolecular 5-*enolexo* aldolization of 1,6-dicarbonyl compounds were fully rationalized using density functional theory methods. A polarizable continuum model was used to describe solvent effects. While 6-*enolexo* aldolizations are well described by Houk's model on the basis of steric and electrostatic contacts, the main factors conditioning the final selectivity in 5-*enolexo* processes are calculated to be quite different. Thus, the selectivity results from the summation of several small electrostatic contacts with an unexpected HOMO electronic overlapping plus the ring strain of the five-membered ring, whereas steric effects seem to be unimportant. Our results indicate, in contrast with 6-*enolexo* processes, that high selectivities are not expected in this type of reaction and that the experimental selectivity shall be very dependent on the reaction conditions, as known experimental results seem to suggest. 7-*enolendo* products are not expected, as they are predicted to be formed by higher energetic transition states. Variable reaction rates, experimentally observed with different catalysts, are suggested to be mainly a result of different catalyst solubilities.

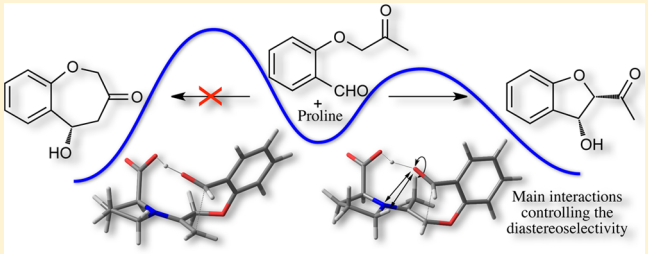

INTRODUCTION

Chiral functionalized cyclopentane rings with or without heteroatoms in the cyclopentane unit, are very important families of compounds that participate in a large variety of naturally occurring structures[1−3] and also in many natural[4,5] and synthetic[6−10] drugs successfully used in the treatment of various diseases.

Many synthetic strategies are known for the preparation of chiral five-membered rings, but most of them rely on the transformation of naturally occurring chiral precursors that, in many cases, are not readily available or have to be submitted to difficult and elaborated transformations.[11−14] One of these approaches[13,14] relies on the intramolecular aldol condensation of dialdehydes catalyzed by amines or ammonium salts, which affords cyclopentene rings in good yield. Even knowing that dialdehydes could, indeed, undergo amine-catalyzed intramolecular aldol condensations, its chiral version, by using chiral amines as catalysts, revealed to be a difficult task, as the obtained selectivities were quite low.[15−17] A pioneering effort was made by Kurteva and Afonso[16] on the 5-*enolexo* aldol condensation of *meso*-3,4-disubstituted-1,6-dialdehydes (Scheme 1). Two different dialdehydes were tested with several amine catalysts, some of them known to afford very good selectivities in 6-*enolexo* and 6-*enolendo* condensations,[15,18,19] but only low to medium yields and selectivities were obtained. However, Enders et al. published in 2005 a very interesting report where the synthesis of *cis*-substituted dihydrobenzofuranols via intramolecular asymmetric organocatalytic 5-*enolexo* aldol reactions was described (Scheme 1).[20] More recently, Hayashi et al. published a similar approach, by using 2-(pyrrolidinylmethyl)pyrrolidine as catalyst (Scheme 1).[21] In both cases, good yields and selectivities were obtained, in apparent contrast with the previous reports. Baati et al. also published an interesting work on 5- and 6-*enolexo* aldolizations, but they were mainly interested in the reaction chemoselectivity, when 1,6- and 1,7-ketoaldehydes are used.[22] The obtained results have been later rationalized in a copublication with Himo et al.[23]

Because of the large number of experimental papers on catalytic 6-*enolendo* and 6-*enolexo* aldolcyclizations, it is natural that the theoretical studies aiming at the rationalization of the experimental selectivities are all based on these systems.[24] After a long, intense, and interesting discussion, and after several mechanism proposals that were aimed at the rationalization of the experimental observations,[25] Houk et al. made a proposal, as described in Scheme 2,[26−30] that is now generally accepted by the scientific community. This mechanism involves an enamine intermediate, followed by a transition state with concerted C−C bond formation and proton transfer from the carboxylic acid group to the carbonyl acceptor. The proposal was then applied by List et al. for 6-*enolexo* processes[31] and later generalized to a broad number of situations.[24] Contrasting with this large amount of information, the rationalization of the selectivities obtained in 5-*enolexo* aldol reactions was never achieved. Thus, in this paper, we aim at the rationalization of the experimental results obtained

Received: March 29, 2012
Published: May 31, 2012

   dx.doi.org/10.1021/jo300633y | *J. Org. Chem.* 2012, 77, 5569−5576

Scheme 1. Reported Results by Kurteva and Afonso,[16] Enders et al.,[20] and Hayashi et al.[21] on Chiral Catalyzed 5-*enolexo* Aldolizations

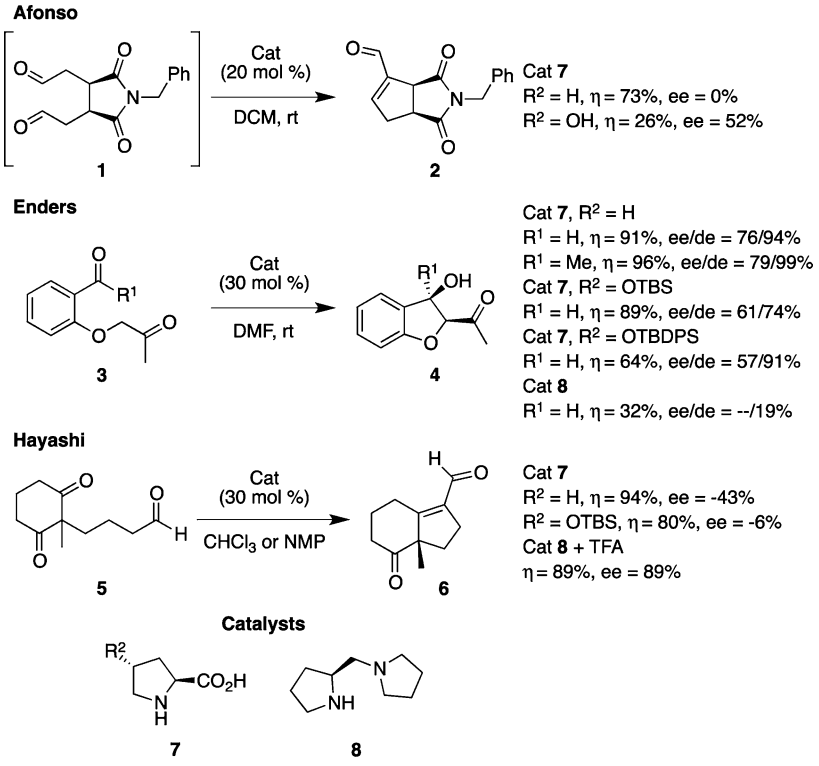

Scheme 2. Proposed Mechanisms for *enolendo*[26−30] and *enolexo*[31] Intramolecular Adol Reactions Catalyzed by Proline

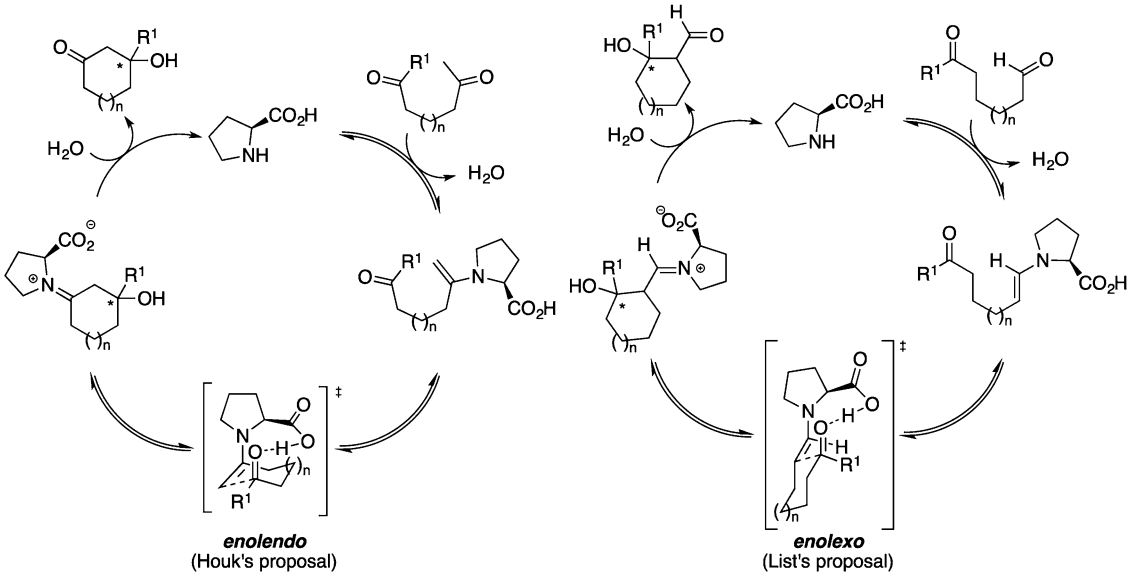

by Enders et al.[20] and at the comparison of our proposals with the models accepted for 6-*enolendo* and 6-*enolexo* processes, in order to establish differences and similarities that can influence the design of catalysts and substrates. Selected results obtained by Kurteva and Afonso[16] will be also analyzed, in order to understand the apparent large discrepancy with the results from Enders et al.[20] and Hayashi et al.[21]

RESULTS AND DISCUSSION

Enders and co-workers reported a proline-catalyzed asymmetric intramolecular *cis*-5-*enolexo* aldolization of several ketoaldehydes and diketones (**3**), to afford the respective 2,3-dihydrobenzofuranols (**4**) (Scheme 3).[20] Several catalysts were tested, with the best results obtained for proline and some proline derivatives (Scheme 3 and Table 1), and the selectivities have been rationalized according to the model proposed by Houk et al. (Scheme 2).[26] Although the diastereo- and enantioselectivities obtained with proton donor catalysts were similar, the reaction rates were strongly dependent on the catalyst (Table 1). Catalysts without proton donor ability were totally inefficient, a result that strongly supports the validity of Houk's model. We will not discuss those catalysts here. When diketones were used

dx.doi.org/10.1021/jo300633y | J. Org. Chem. 2012, 77, 5569−5576

Scheme 3. Chiral Amine-Catalyzed 5-*enolexo* Aldolizations of Dicarbonylic Compounds[20]

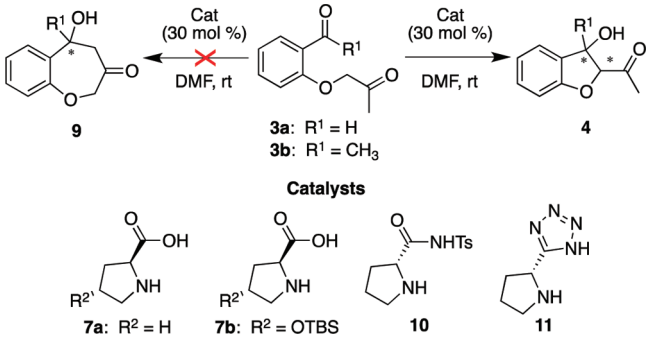

instead of ketoaldehydes, a substantial improvement on the reaction diastereoselectivity was observed while the enantioselectivity did not change much (Table 1, last entry). In no case was observed the formation of 7-*enolendo* products (Scheme 3, structure **9**).

Recently, we reported that the rate-limiting step in catalytic 6-*enolexo* aldol condensations of 1,7-dicarbonylic compounds can be either the initial attack of the catalyst to the carbonyl group or the iminium formation step,[32] a result that is in full agreement with kinetic studies reported by Meyer et al.[33] Thus, in order to rationalize the large variation of the reaction rates reported by Enders et al., it is necessary to evaluate not only the activation energies of the cyclization TSs but also the activation energies of the enamine formation steps. As these types of structures were already discussed in detail,[32,34] only a general scheme is presented (Scheme 4), the main values being compiled in Table 2 (full data are given in the Supporting Information). For an easy comparison with the experimental results, the calculated selectivities for the cyclization step are already given in Table 1. This discussion is based on results obtained with PBE1PBE/6-31+G**, but all important TS structures are also verified by data obtained with other theoretical models (see the Supporting Information). All structures were calculated with the pyrrolidine ring of the catalyst in its lower-energy conformation.[26,32] The inclusion of the other possible TSs does not change the calculated selectivities, as seen in the Supporting Information when the catalyst is proline.

Several important conclusions can be derived from the data in Table 2. Thus, the activation energies for the cyclization step (**TS-6**) are indeed slightly dependent on the catalyst. While proline and its substituted sililoxy derivative **7b** originate very similar values, the tosyl derivative **10** catalyzes the cyclization with a slightly lower activation energy (reduction of ca. 8 kJ mol^{-1}) and catalyst **11** induces a reduction of ca. 20 kJ mol^{-1} (comparison with proline). On the other hand, with the exception of catalyst **11**, the rate-limiting step is the dehydration step (**TS-2**), in agreement with previous results.[32,34] With

Scheme 4. General Proposed Reaction Pathway for the Formation of 5-*enolexo* Products in the Reaction Reported by Enders et al.[20a]

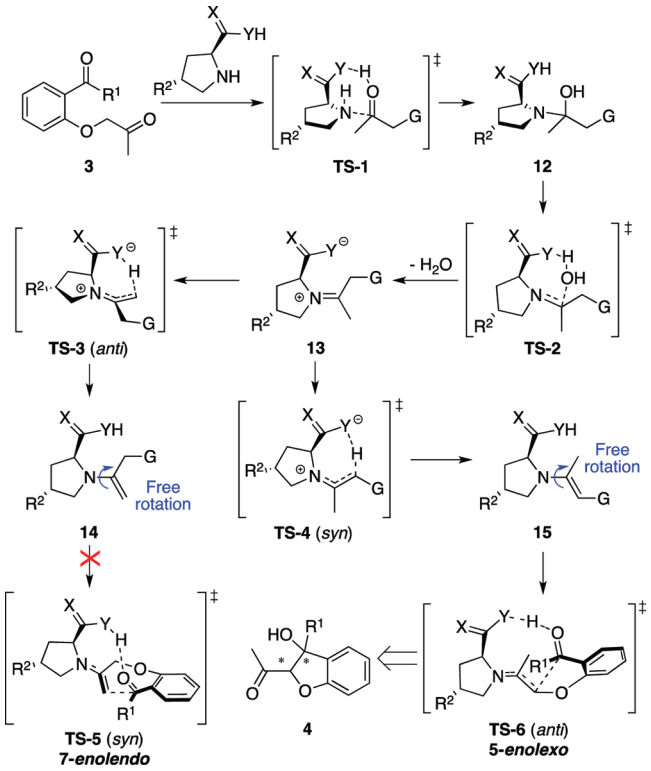

[a]Energy values are given in Table 2.

catalyst **11**, the rate-limiting step is the enamine formation (but almost isoenergetic with **TS-2**), which correlates with the relative acidities of the different tested catalysts (see the Supporting Information). The acid strength of the catalyst is mainly important in **TS-2** and **TS-6**, as the acid has to protonate the oxygen atom, reducing its negative charge. Thus, stronger acids reduce the activation energies of these two TSs. On the other hand, a stronger acid is associated with a weaker conjugated base, which renders the proton removal in **TS-4** more difficult. When the reaction is catalyzed by catalyst **11**, the overall result is a decrease of the activation energy of **TS-2** and **TS-6**, while the activation energy of **TS-4** slightly increases, becoming the rate-limiting step.

If the activation energies associated with the rate-limiting steps calculated for each catalyst are compared, we have to conclude that no important variations of the reaction rates should be observed, as the major difference is only ca. 7 kJ mol^{-1} (between catalysts **11** and **7a**). Thus, we believe that the main reason for the different experimental reaction rates is not their relative activation energies, but the relative solubilities of the catalysts.

Table 1. Main Experimental Results Reported by Enders et al.[20a]

entry	dicarbonyl	catalyst	time	yield (%)	ee (%)	de (%)	config
1	**3a**	**7a**	24 h	91	76 (82.9)	94 (94.4)	2*S*,3*R*
2	**3a**	**7b**	75 min	89	61 (88.1)	74 (98.6)	2*S*,3*R*
3	**3a**	**10**	3 d	66	77 (82.0)	89 (95.8)	2*R*,3*S*
4	**3a**	**11**	15 h	86	68 (70.9)	96 (78.0)	2*R*,3*S*
5	**3b**	**7a**	20 h	96	73 (97.0)	99 (99.7)	2*S*,3*R*

[a]Calculated stereoselectivities are in parentheses.

dx.doi.org/10.1021/jo300633y | J. Org. Chem. 2012, 77, 5569−5576

Table 2. Gibbs Activation Energy Values Calculated for the Main Steps Presented in Scheme 4, with Four Different Catalysts (See Scheme 3)[a]

		Catalyst							
		7a		7b		10		11	
entry	(R^1 = H)	*syn*	*anti*	*syn*	*anti*	*syn*	*anti*	*syn*	*anti*
1	**TS-1**	89.2	88.6	92.1	90.7	92.4	90.2	74.7	70.6
2	**TS-2**	96.3	97.7	95.1	97.0	93.2	93.7	84.8	85.0
3	**TS-3**	152.3	95.1	156.0	99.2	144.7	92.1	147.3	95.6
4	**TS-4**	86.5	140.5	91.0	142.2	82.6	127.2	88.9	135.1
5	**TS-5**	115.2	142.0						
6	**TS-6**	85.2	79.3	85.2	78.3	77.1	71.5	63.5	59.1

[a]Only the two lowest-energy values are given for **TS-6**. Full data are given in the Supporting Information. Energies are in kJ mol^{-1}.

Indeed, while catalyst **7b** induces, in all reaction steps, similar activation energies as proline, it originates the highest reaction rate, just because **7b** is much more soluble than proline.

Enders et al.[20] did not observe the formation of 7-*enolendo* cyclization products, a result that is explained by the large activation energy calculated for the cyclization step (**TS-5**, Scheme 4 and Table 2). As **TS-5** is the rate-limiting step in this reaction pathway and as all the previous steps are reversible, the cyclization follows the lowest-energy pathway, originating exclusively 5-*enolexo* products.

We have previously applied Houk's model[26] to the rationalization of the experimental selectivities observed by List et al.[31] in 6-*enolexo* aldolcyclizations of 1,7-dicarbonylic compounds,[32,35] and we were able to identify the main molecular interactions that are responsible for the observed selectivities. Thus, while the high enantioselectivities mainly originate from different electrostatic interactions between the forming alkoxy group and one of the α-hydrogen atoms in the proline ring, the calculated diastereoselectivities result from different steric contacts in the equatorial and axial orientations of the proline moiety in the TS structures (Figure 1). Enders et al. proposed a similar TS to rationalize the experimental observed selectivities. However, important differences have to exist because while the enantioselectivities obtained by Enders et al.[20] and also by Hayashi et al.[21] in 5-*enolexo* aldolizations are considerably higher than those previously obtained by Kurteva and Afonso,[16] they are, however, considerably lower than those obtained by List et al. in 6-*enolexo* aldolizations.[31] Also, the absolute configurations obtained by Enders et al. are different from those obtained by List et al.

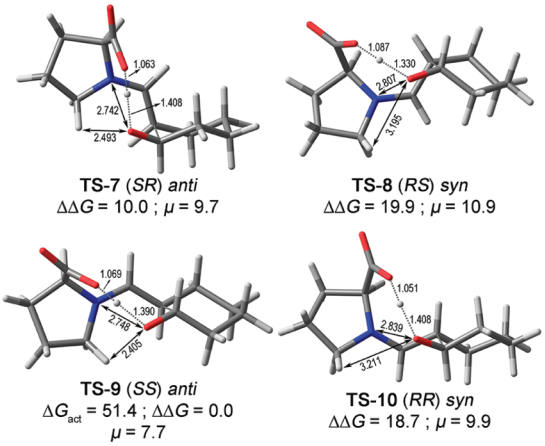

Figure 1. Calculated TS structures for the 6-*enolexo* cyclization of 1,7-heptanedial catalyzed by (*S*)-proline.[32,36] All bond lengths are in angstroms (Å), energies in kJ mol^{-1}, and dipole moments in Debye (D).

Figure 2 displays the four TS structures for the cyclization of ketoaldehyde **3a** catalyzed by proline, as well as their relative activation energies. The comparison of Figures 1 and 2 raises three simple conclusions that are in full agreement with the experimental data. While proline preferentially induces the formation of isomer *SS* in 6-*enolexo* aldolizations (Figure 1), isomer *SR* is preferentially formed in 5-*enolexo* processes (Figure 2). While, in 6-*enolexo* reactions, the enantioselectivity is calculated to be substantially higher than the diastereoselectivity, the opposite is true in 5-*enolexo* processes. While in 6-*enolexo* aldolizations, the calculations predict high enantioelectivity ($\Delta\Delta G \approx 20$ kJ mol^{-1}), in 5-*enolexo* reactions, only modest selectivity is expected ($\Delta\Delta G \approx 6$ kJ mol^{-1}). Thus, from the observed differences between Figures 1 and 2, it seems, indeed, that different phenomena are involved in the two compared aldolization processes.

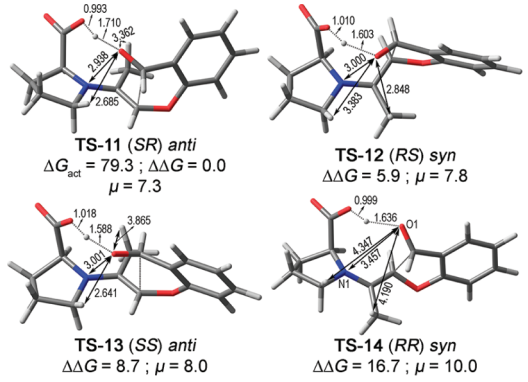

Figure 2. Calculated TS structures for the 5-*enolexo* cyclization of compound **3a** catalyzed by (*S*)-proline. Bond lengths are in angstroms (Å), energies in kJ mol^{-1}, and dipole moments in Debye (D).

The conformational equilibrium between the *syn*- and *anti*-enamines (structure **15** in Scheme 4) is known to be a fast process,[32,34,37] thus not influencing the final selectivity. However, it is acceptable to think that, since **TS-11** (*SR*) and **TS-13** (*SS*) are both resultant from the enamine *anti* conformation and **TS-12** (*RS*) and **TS-14** (*RR*) are both resultant from the enamine *syn* conformation, any energy difference observed between the two enamine conformers is also reflected in the energy of the resulting TSs. This is indeed an important factor when catalysts with larger groups in the pyrrolidine moiety are used.[34] However, proline and other proline derivatives with small substituent groups do not induce any important energy difference between

dx.doi.org/10.1021/jo300633y | J. Org. Chem. 2012, 77, 5569−5576

the two enamine conformers, in enamines resulting from either aldehydes or ketones (Scheme 3).[32] Thus, in Figure 1, the steric effects result from the equatorial versus axial conformation of the catalyst moiety and not from the *syn*/*anti* orientation of the enamine bond. In the structures in Figure 2, there is also the possibility of equatorial/axial orientations (see the Supporting Information for a different perspective of the four TSs). However, apparently, they do not influence the activation energy of the TSs. Indeed, while **TS-11** (*SR*) has the proline moiety in an axial orientation, it has also the lowest activation energy. On the other hand, **TS-14** (*RR*) has the proline moiety in an equatorial orientation, but it shows the highest activation energy. Thus, if steric effects seem to be unimportant in the definition of the reaction selectivity, we have to turn our attention to electrostatic and electronic effects.

In 6-*enolexo* reactions, the enantioselectivity mainly results from electrostatic interactions between the forming alkoxy group and one of the α-hydrogen atoms in the proline ring (Figure 1).[32,35] Similar interactions can be observed in Figure 2, albeit slightly weaker, as the distances are larger than those in Figure 1. The data in Figure 2 also indicate that these interactions alone cannot justify the relative activation energies of the four TSs. Indeed, in **TS-12** (*RS*), the distance between the two atoms is larger than in **TS-13** (*SS*), but the energy is lower in the first. However, a second interaction is observed in **TS-12** (*RS*) between the forming alkoxy group and one of the methyl hydrogen atoms, which can contribute to reduce its energy. In the other structures, the same interaction is considerably weaker, as the distances are at least 1 Å longer. When the methyl group is replaced by hydrogen, the predicted energy difference between isomers *SR* and *RS* increases in ca. 1 kJ mol^{-1}, which shows the importance of this contact (see the Supporting Information). However, there is another interaction that also contributes to the calculated selectivities. In the cyclization transition state, there is charge transfer from the enamine nitrogen atom (N1, Figure 2) to the carbonyl atom (O1, Figure 2). Therefore, the enamine nitrogen atom acquires iminium character, becoming positively charged, while the oxygen atom in the carbonyl group becomes negatively charged (see the Supporting Information, Figure S5). This negative charge needs to be stabilized by hydrogen bond contacts, as those discussed above. However, the two opposite charges in the nitrogen and oxygen atoms can be mutually stabilized, as the distance between them is short. In fact, the shortest distance is observed in **TS-11** (*SR*), the most stable TS. **TS-12** (*RS*) and **TS-13** (*SS*) have similar distances and similar energies, whereas **TS-14** (*RR*) has the largest distance and the largest activation energy value. The interaction between the nitrogen and the oxygen atoms is not only of electrostatic type. In fact, the HOMO orbitals in all TSs have the proper symmetry to establish in-phase overlapping between p orbitals of these two atoms, but the importance of these interactions diminishes as the distance between the two atoms increases (Figure 3). This effect is reflected in the relative dipolar moments of the four TSs, thus originating good correlation between the relative activation energies and the calculated dipolar moments (Figure 2). If we look for similar contacts in 6-*enolexo* processes (Figure 1), we have to conclude that they are unimportant in the establishment of the final selectivities, as the contact distances are very similar in the four structures. Resuming, while in 6-*enolexo* processes, the calculated selectivity results from steric and electrostatic effects in the TS structures, in 5-*enolexo* reactions, the main factors controlling the selectivity are of electrostatic and an electronic nature. In contrast with the 6-*enolexo* cyclizations, the forming

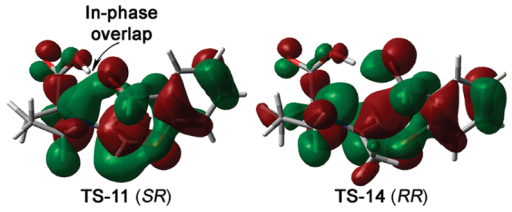

Figure 3. HOMO orbitals calculated for **TS-11** and **TS-14**, showing the strong in-phase overlapping between the nitrogen and the oxygen (carbonyl group) atoms in **TS-11**. Isosurfaces at 0.02 au.

five-membered ring is a substantially more rigid structure that does not allow all the TSs to relax to conformations that maximize the electrostatic and electronic contacts. It is then reasonable to expect that this type of reactions are more sensitive to the reaction media, as solvent polarity, pH, and temperature can all strongly affect the efficiency of the phenomena controlling the selectivity. Steric effects, by their nature, are less prone to be affected by these reaction variables.

All the discussion above was done with proline as the catalyst. However, the behavior of the other three studied catalysts is, with a few exceptions, very similar to that discussed for proline, thus originating also similar calculated selectivities (Table 1). In the case of catalyst **10**, we had to calculate the selectivities by Boltzmann averaging of eight structures, due to two possible conformers of the tosyl group in each TS. For this catalyst, it is also not possible to correlate the dipole moments with the relative energies, as the electronegative tosyl group strongly influences the dipole moments, resulting all in very similar values.

Enders et al.[20] also observed that the use of diketones instead of ketoaldehydes improves the diastereoselectivity while keeping the enantioselectivity. By analyzing the structures in Figure 2, this result is not unexpected. Indeed, in each pair of enantiomers, the extra methyl group has to adopt the same orientation, in relation to the initial methyl group. However, while in the enantiomeric pair *SR*/*RS*, the two methyl groups have to adopt an *anti* orientation, thus not originating steric repulsion between them, in the enantiomeric pair *SS*/*RR*, the methyl groups have to adopt a *syn* orientation, which originates steric repulsion with a consequent increase in the activation energy. We calculated the four TS structures for the cyclization of diketone **3b** (Figure 4), and we indeed conclude that the energy difference between the two pairs of enantiomers substantially increases (in fact, it doubles), thus originating an improvement in the diastereose-

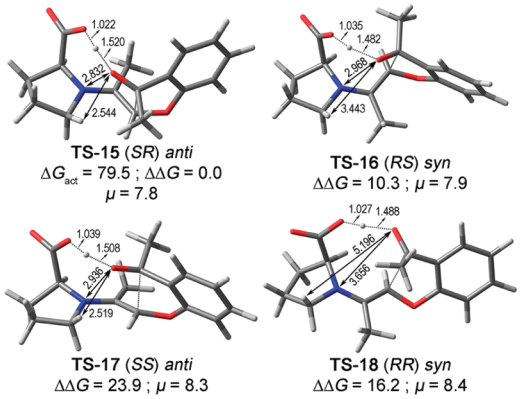

Figure 4. Calculated TS structures for the 5-*enolexo* cyclization of compound **3b** catalyzed by (*S*)-proline. All bond lengths are in angstroms (Å), energies in kJ mol^{-1}, and dipole moments in Debye (D).

dx.doi.org/10.1021/jo300633y | J. Org. Chem. 2012, 77, 5569−5576

lectivity, while the energy difference between each enantiomer increases much less. Even so, the result is a small improvement in the enantioselectivity, which is not in full agreement with the experiment. It seems that this is not a theoretical model issue, as we tested the system with several models and all of them originated similar results (see the Supporting Information).

Considering the previous discussion, we should now be able to rationalize the low selectivities obtained by Kurteva and Afonso in their pioneering work.[16] We calculated all the structures in their approach, using proline as catalyst, and the results are in Scheme 5. The data in Scheme 5 indicates that the rate-limiting steps are also the initial amine attack to the aldehyde (**TS-19**, *RS* pathway) or the iminium formation step (**TS-22**, *SR* pathway). However, while in the system from Enders et al.[20] and in the system from Hayashi et al.[21] the two or three carbonyl groups that can potentially react with the amine catalyst to form the enamine intermediate are of quite different reactivities, leading to a single enamine intermediate, Kurteva and Afonso used *meso*-dialdehydes that have very similar carbonyl groups and form two diastereomeric enamine intermediates in low diastereoselectivity. This apparently unimportant difference is, in fact, responsible for the low selectivities obtained by Kurteva and Afonso. Indeed, the cyclization step, which is similar to that calculated for the pathway from Enders et al., originates also medium selectivities (albeit leading to eight diastereomers). However, the selectivity induced in the cyclization step is irrelevant for the final reaction selectivity, as the two chiral centers are destroyed in the following water elimination step (Scheme 5). Thus, the final reaction enantioselectivity results only from the two initial reaction steps (**TS-19** and **TS-22**), which originate low selectivity, as was discussed above. This conclusion answers the question raised by List et al.,[15] who wondered why Kurteva and Afonso[16] were unable to reach high selectivities in 5-*enolexo* aldol condensations catalyzed by proline, a catalyst that performs quite well in this type of transformation. Proline can, indeed, perform well in the cyclization step, albeit substantially worse than in 6-*enolexo* processes, but there is no apparent reason to induce high selectivity in the initial reaction steps when *meso*-dicarbonyl compounds are used. A similar conclusion was previously reported by us,[32] when we studied the 6-*enolexo* aldolization of *meso*-1,7-dicarbonylic compounds reported by List et al.[31]

Considering the very similar activation energies calculated for the first and second steps of the system from Kurteva and Afonso, the low, but different, selectivities he obtained with different catalysts can, eventually, be attributed to experimental issues, (pH, solvent effects, etc.) as it is well known that the performance of proline-derived catalysts is extremely dependent on the reaction conditions.[19,22,38,39] The results obtained by Baati et al.[22] in 5-*enolexo* aldolizations of 1,6-ketoaldehydes catalyzed by proline, in which different chemoselectivities were obtained depending on the solvent, are an important support to our suggestion.

CONCLUSIONS

The experimental diastereoselectivity obtained by Enders et al. in the amine-catalyzed intramolecular 5-*enolexo* aldolizations of 1,6-dicarbonyl compounds was, for the first time, fully rationalized. We used Houk's model properly adapted for 5-*enolexo* systems, and we found that the origins of the selectivity are quite different from those identified for 6-*enolexo* cyclizations. While in 6-*enolexo* aldolizations, the high enantioselectivities mainly originate from different electrostatic interactions between the forming alkoxy group and one of the α-hydrogen atoms in the proline ring, and the calculated diastereoselectivities result from different steric contacts in the equatorial versus axial orientation of the proline moiety in the TS structures, in 5-*enolexo* aldolizations, the selectivity results from the summation of several small electrostatic contacts with an unexpected HOMO

Scheme 5. Calculated Relative Energy Values and Selectivities in the Proline-Catalyzed 5-*enolexo* Aldol Condensation of *meso*-3,4-Disubstituted-1,6-dialdehydes, Reported by Kurteva and Afonso[16a]

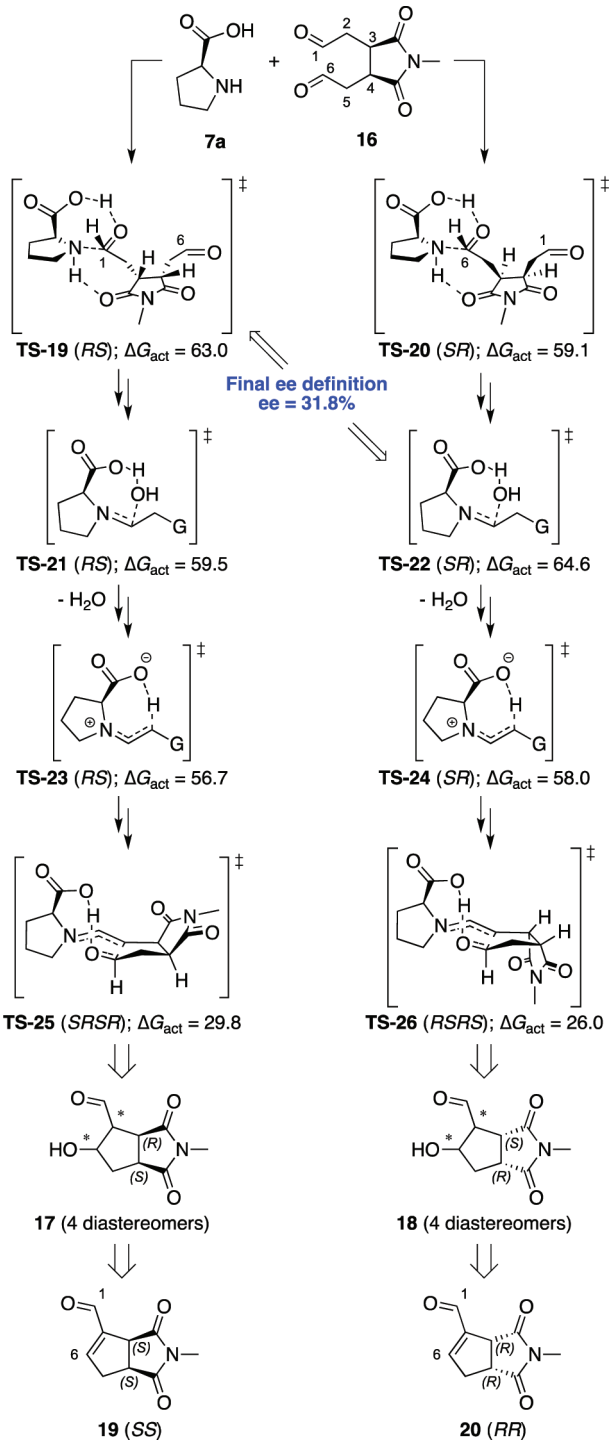

[a]The final selectivity is calculated between **TS-19** and **TS-22**, which are the rate-limiting steps for each reaction pathway. Energies are in kJ mol^{-1}.

dx.doi.org/10.1021/jo300633y | J. Org. Chem. 2012, 77, 5569−5576

electronic overlapping plus the ring strain of the five-membered ring, while steric effects become important only when the substrate is a diketone. Our results indicate, in contrast with 6-*enolexo* processes, that high selectivities are not expected in this type of reaction and that the experimental selectivity shall be very dependent on the reaction conditions. 7-*enolendo* products are not expected, as they are predicted to be formed by higher energetic transition states. Variable reaction rates, experimentally observed with different catalysts, are suggested to be mainly a result of different catalyst solubilities.

COMPUTATIONAL METHODS

Full geometry optimizations have been performed with the Gaussian 09, revision B.01, software package[40] employing density functional theory (DFT)[41,42] with the hybrid functional PBE1PBE[43−46] and the 6-31+G** basis set. Solvent effects in DMF were included in the optimizations by using the polarizable continuum model (PCM).[47] The structures in Scheme 5 where calculated with dichloromethane, as this was the solvent used in the experiments. Harmonic vibrational frequencies have been calculated for all located stationary structures to verify whether they are minima or transition states. Zero-point energies and thermal corrections have been taken from unscaled vibrational frequencies. Free energies of activation are given at 25 °C. The energy values of all relevant TSs have been refined by single-point PCM DFT calculations at PBE1PBE/6-311+G** and M06-2X/6-311+G**[48] levels of theory, over the optimized PCM PBE1PBE/6-31+G** geometries, and single-point PCM DFT calculations at the B3LYP/6-311+G**[49] level of theory, over the optimized PCM B3LYP/6-31+G** geometries (all values are given in the Supporting Information). The four cyclization TSs of compound **3b** (Figure 4) were also optimized with PCM DFT ωB97XD/6-31+G**[50] and LC-ωPBE/6-31+G**[51−54] (see the Supporting Information). All energies are calculated relative to the reagents. All bond lengths are in angstroms (Å), energies in kJ mol^{-1}, and dipole moments in Debye (D).

ASSOCIATED CONTENT

Supporting Information

Cartesian coordinate matrixes, electronic energies, and thermal corrections of all calculated structures. This material is available free of charge via the Internet at http://pubs.acs.org.

AUTHOR INFORMATION

Corresponding Author

*E-mail: ags@fct.unl.pt.

Notes

The authors declare no competing financial interest.

ACKNOWLEDGMENTS

We are grateful to the Fundação para a Ciência e Tecnologia (SFRH/BPD/22179/2005 and PTDC/QUI-QUI/104056/2008) for financial support.

REFERENCES

(1) Khanum, S. A.; Shashikanth, S.; Sudha, B. S.; Sriharsha, S. N. *J. Chem. Res., Synop.* **2003**, 463−464.
(2) Zou, Y.; Lobera, M.; Snider, B. B. *J. Org. Chem.* **2005**, *70*, 1761−1770.
(3) Jiménez, B.; Grande, M. C.; Anaya, J.; Torres, P.; Grande, M. *Phytochemistry* **2000**, *53*, 1025−1031.
(4) Kusaka, T.; Yamamoto, H.; Shibata, M.; Muroi, M.; Kishi, T.; Mizuno, K. *J. Antibiot.* **1968**, *21*, 255−263.
(5) Yaginuma, S.; Muto, N.; Tsujino, M.; Sudate, Y.; Hayashi, M.; Otani, M. *J. Antibiot.* **1981**, *34*, 359−366.
(6) Vince, R.; Hua, M. *J. Med. Chem.* **1990**, *33*, 17−21.
(7) Jones, M.; Myers, P.; Robertson, C.; Storer, R.; Williamson, C. *J. Chem. Soc., Perkin Trans. 1* **1991**, 2479−2484.
(8) Trost, B.; Madsen, R.; Guile, S.; Brown, B. *J. Am. Chem. Soc.* **2000**, *122*, 5947−5956.
(9) Crimmins, M.; King, B. *J. Org. Chem.* **1996**, *61*, 4192−4193.
(10) Foster, R.; Faulds, D. *Drugs* **1998**, 729−736.
(11) White, J. D. *Synthesis* **1998**, 619−626.
(12) Corey, E. J.; Desai, M. C.; Engler, T. A. *J. Am. Chem. Soc.* **1985**, *107*, 4339−4341.
(13) Maycock, C. D.; Barros, M. T.; Santos, A. G.; Godinho, L. S. *Tetrahedron Lett.* **1993**, *34*, 7985−7988.
(14) Maycock, C. D.; Barros, M. T.; Santos, A. G.; Godinho, L. S. *Tetrahedron Lett.* **1994**, *35*, 3999−4002.
(15) Mukherjee, S.; Yang, J. W.; Hoffmann, S.; List, B. *Chem. Rev.* **2007**, *107*, 5471−5569.
(16) Kurteva, V. B.; Afonso, C. A. M. *Tetrahedron* **2005**, *61*, 267−273.
(17) Ghobril, C.; Sabot, C.; Mioskowski, C.; Baati, R. *Eur. J. Org. Chem.* **2008**, 4104−4108.
(18) Moyano, A.; Rios, R. *Chem. Rev.* **2011**, *111*, 4703−4832.
(19) Giacalone, F.; Gruttadauria, M.; Agrigento, P.; Noto, R. *Chem. Soc. Rev.* **2012**, *41*, 2406−2447.
(20) Enders, D.; Niemeier, O.; Straver, S. *Synlett* **2006**, 3399−3402.
(21) Hayashi, Y.; Sekizawa, H.; Yamaguchi, J.; Gotoh, H. *J. Org. Chem.* **2007**, *72*, 6493−6499.
(22) Ghobril, C.; Sabot, C.; Mioskowski, C.; Baati, R. *Eur. J. Org. Chem.* **2008**, 4104−4108.
(23) Hammar, P.; Ghobril, C.; Antheaume, C.; Wagner, A.; Sabot, C.; Baati, R.; Himo, F. *J. Org. Chem.* **2010**, *75*, 4728−4736.
(24) Cheong, P. H.-Y.; Legault, C. Y.; Um, J. M.; Çelebi-Ölçüm, N.; Houk, K. N. *Chem. Rev.* **2011**, *111*, 5042−5137.
(25) Hoang, L.; Bahmanyar, S.; Houk, K. N.; List, B. *J. Am. Chem. Soc.* **2003**, *125*, 16−17.
(26) Clemente, F. R.; Houk, K. N. *Angew. Chem., Int. Ed.* **2004**, *43*, 5766−5768.
(27) Allemann, C.; Gordillo, R.; Clemente, F. R.; Cheong, P. H. Y.; Houk, K. N. *Acc. Chem. Res.* **2004**, *37*, 558−569.
(28) Bahmanyar, S.; Houk, K. N. *J. Am. Chem. Soc.* **2001**, *123*, 12911−12912.
(29) Bahmanyar, S.; Houk, K. N. *J. Am. Chem. Soc.* **2001**, *123*, 11273−11283.
(30) Clemente, F. R.; Houk, K. N. *J. Am. Chem. Soc.* **2005**, *127*, 11294−11302.
(31) Pidathala, C.; Hoang, L.; Vignola, N.; List, B. *Angew. Chem., Int. Ed.* **2003**, *42*, 2785−2788.
(32) Duarte, F. J. S.; Cabrita, E. J.; Frenking, G.; Santos, A. G. *J. Org. Chem.* **2010**, *75*, 2546−2555.
(33) Zhu, H.; Clemente, F. R.; Houk, K. N.; Meyer, M. P. *J. Am. Chem. Soc.* **2009**, *131*, 1632−1633.
(34) Duarte, F. J. S.; Santos, A. G. *J. Org. Chem.* **2012**, *77*, 3252−3261.
(35) Duarte, F. J. S.; Cabrita, E. J.; Frenking, G.; Santos, A. G. *Eur. J. Org. Chem.* **2008**, 3397−3402.
(36) These structures were reoptimized with the same theoretical model we used in this paper, to allow for a proper comparison.
(37) Schmid, M. B.; Zeitler, K.; Gschwind, R. M. *Angew. Chem., Int. Ed.* **2010**, *49*, 4997−5003.
(38) Hayashi, Y.; Sumiya, T.; Takahashi, J.; Gotoh, H.; Urushima, T.; Shoji, M. *Angew. Chem., Int. Ed.* **2006**, *45*, 958−961.
(39) Aratake, S.; Itoh, T.; Okano, T.; Nagae, N.; Sumiya, T.; Shoji, M.; Hayashi, Y. *Chem.—Eur. J.* **2007**, *13*, 10246−10256.
(40) Frisch, M. J.; Trucks, G. W.; Schlegel, H. B.; Scuseria, G. E.; Robb, M. A.; Cheeseman, J. R.; Scalmani, G.; Barone, V.; Mennucci, B.; Petersson, G. A.; Nakatsuji, H.; Caricato, M.; Li, X.; Hratchian, H. P.; Izmaylov, A. F.; Bloino, J.; Zheng, G.; Sonnenberg, J. L.; Hada, M.; Ehara, M.; Toyota, K.; Fukuda, R.; Hasegawa, J.; Ishida, M.; Nakajima, T.; Honda, Y.; Kitao, O.; Nakai, H.; Vreven, T.; Montgomery, J. A., Jr.; Peralta, J. E.; Ogliaro, F.; Bearpark, M.; Heyd, J. J.; Brothers, E.; Kudin, K. N.; Staroverov, V. N.; Kobayashi, R.; Normand, J.; Raghavachari, K.; Rendell, A.; Burant, J. C.; Iyengar, S. S.; Tomasi, J.; Cossi, M.; Rega, N.; Millam, J. M.; Klene, M.; Knox, J. E.; Cross, J. B.; Bakken, V.; Adamo, C.;

Jaramillo, J.; Gomperts, R.; Stratmann, R. E.; Yazyev, O.; Austin, A. J.; Cammi, R.; Pomelli, C.; Ochterski, J. W.; Martin, R. L.; Morokuma, K.; Zakrzewski, V. G.; Voth, G. A.; Salvador, P.; Dannenberg, J. J.; Dapprich, S.; Daniels, A. D.; Farkas, O.; Foresman, J. B.; Ortiz, J. V.; Cioslowski, J.; Fox, D. J. *Gaussian 09*, revision B.01; Gaussian, Inc.: Wallingford, CT, 2009.
(41) Koch, W.; Holthausen, M. C. *A Chemist's Guide to Density Functional Theory*, 2nd ed.; Wiley: New York, 2001.
(42) Parr, R. G.; Yang, W. *Density Functional Theory of Atoms and Molecules*; Oxford University Press: Oxford, U.K., 1989.
(43) Perdew, J. P.; Burke, K.; Ernzerhof, M. *Phys. Rev. Lett.* **1996**, *77*, 3865−3868.
(44) Perdew, J. P.; Burke, K.; Ernzerhof, M. *Phys. Rev. Lett.* **1997**, *78*, 1396−1396.
(45) Adamo, C.; Barone, V. *J. Chem. Phys.* **1999**, *110*, 6158−6169.
(46) Wheeler, S. E.; Moran, A.; Pieniazek, S. N.; Houk, K. N. *J. Phys. Chem. A* **2009**, *113*, 10376−10384.
(47) Tomasi, J.; Mennucci, B.; Cammi, R. *Chem. Rev.* **2005**, *105*, 2999−3093.
(48) Zhao, Y.; Truhlar, D. G. *Theor. Chem. Acc.* **2008**, *120*, 215−241.
(49) Zhang, Y.; Xu, X.; Goddard, W. A., III *Proc. Natl. Acad. Sci. U.S.A.* **2009**, *106*, 4963−4968.
(50) Chai, J.-D.; Head-Gordon, M. *Phys. Chem. Chem. Phys.* **2008**, *10*, 6615−6620.
(51) Tawada, Y.; Tsuneda, T.; Yanagisawa, S.; Yanai, T.; Hirao, K. *J. Chem. Phys.* **2004**, *120*, 8425−8433.
(52) Vydrov, O. A.; Scuseria, G. E. *J. Chem. Phys.* **2006**, *125*, 234109.
(53) Vydrov, O. A.; Heyd, J.; Krukau, A.; Scuseria, G. E. *J. Chem. Phys.* **2006**, *125*, 074106.
(54) Vydrov, O. A.; Scuseria, G. E.; Perdew, J. P. *J. Chem. Phys.* **2007**, *126*, 154109.